WILEY-VCH

Preparation and characterization of mixed halide $MAPbI_{3-x}Cl_x$ perovskite thin films by three-source vacuum deposition.

Azin Babaei, Wiria Soltanpoor, Maria A. Tesa-Serrate, Selcuk Yerci, Michele Sessolo and Henk J. Bolink*

A. Babaei, Dr. M. Sessolo, Prof. H. J. Bolink
Instituto de Ciencia Molecular, Universidad de Valencia, C/Catedratico J. Beltrán 2, 46980 Paterna, Spain. E-mail: michele.sessolo@uv.es

W. Soltanpoor, Prof. S. Yerci
Centre for Solar Energy Research and Applications (GÜNAM), Middle East Technical University, 06800 Ankara, Turkey
Department of Micro and Nanotechnology, Middle East Technical University, 06800 Ankara, Turkey
Department of Electrical and Electronics Engineering, Middle East Technical University, 06800 Ankara, Turkey

Prof. S. Yerci
Department of Electrical and Electronics Engineering, Middle East Technical University, 06800 Ankara, Turkey

Dr. M.A. Tesa-Serrate
Edinburgh Instruments, 2 Bain Square, Kirkton Campus, EH54 7DQ Livingston, United Kingdom

Keywords: halide perovskites, solar cells, vacuum deposition, mixed halide perovskite

Abstract

Chloride has been extensively used in the preparation of metal halide perovskites such as methylammonium lead iodide ($MAPbI_{3-x}Cl_x$), but its persistence and role in solution-processed materials has not yet been rationalized. Multiple-source vacuum deposition of perovskites enables a fine control over the thin-film stoichiometry, and allows to incorporate chemical species irrespectively of their solubility. In this communication, we present the first example of mixed $MAPbI_{3-x}Cl_x$ thin films prepared by three-source vacuum deposition using MAI, PbI_2 and $PbCl_2$ as precursors. The optoelectronic properties of the material are evaluated through photovoltaic and electro-/photo-luminescent characterizations. Besides the very similar structural and optical properties of $MAPbI_3$ and $MAPbI_{3-x}Cl_x$, we observed an increased

electroluminescence efficiency, longer photoluminescence lifetimes, as well as larger photovoltage in the presence of chloride, suggesting a reduction of the non-radiative charge recombination.

Organic-inorganic (hybrid) metal halide perovskites are being studied as promising semiconductors for applications in photovoltaics (PVs) and light-emitting diodes (LEDs), due to their desirable properties, such as high absorption coefficient, long carrier diffusion length and high tolerance to chemical defects.[1–3] The global research efforts resulted in perovskite solar cells with power conversion efficiency (PCE) exceeding 24%,[4] and LEDs with an external quantum efficiency (EQE) of 20%, approaching its theoretical limit.[5–7] In addition, perovskites can be processed into thin films through a variety of low temperature techniques, both from solution and from the vapour phase.[8–10] While most studies have been carried out on solution-processed compounds, likely due to the technical simplicity, vapour phase deposition of perovskites has the advantage of being a solvent-free, intrinsically additive, and scalable process.[9] The archetypal perovskite compound, methylammonium lead iodide ($MAPbI_3$), was initially employed as a mixed halide system with the addition of small amounts of chloride.[11] The mixed halide $MAPbI_{3-x}Cl_x$ was found to have charge diffusion length exceeding 1 μm, about one order of magnitude longer compared to the pure iodide system.[12] Despite many investigations towards the role of chloride, its effect on the optoelectronic properties of MAPI remains poorly understood.[13] Chemical analysis found chloride to be segregated at the interface between $MAPbI_{3-x}Cl_x$ and the electron transport layer (ETL),[14] and in any case its solubility into the triiodide perovskite is extremely small ($x < 0.1$).[15] Interestingly, the first report of vacuum deposited perovskite solar cells used $PbCl_2$ and methylammonium iodide (MAI) as the precursors, resulting in a mixed halide light-absorber.[16] The process used a large excess of MAI ($MAI:PbCl_2 = 4:1$), and a long post-annealing process

(100 °C for 45 min in N_2) was needed in order to achieve full conversion to the perovskite phase. Most of the chloride is indeed lost during conversion of the precursors to the perovskite. In order to circumvent the difficulties of obtaining a stoichiometrically controlled $MAPbI_{3-x}Cl_x$ through vacuum deposition, sequential techniques such as vapour transfer method to convert the inorganic halide,[17] or single source deposition of MAPbCl followed by spin coating of MAI,[18] have also been explored. While technically more demanding, vacuum deposition from multiple sources offers a superior control over the final material stoichiometry, and has been used to prepare mixed halide and mixed cation perovskite thin-films.[19,20] Here we explore the vacuum-deposition of $MAPbI_{3-x}Cl_x$ by co-evaporation of the three precursors, PbI_2, $PbCl_2$ and MAI. Perovskite films with homogenous morphology and high crystallinity are obtained and used in proof-of-concept solar cells with high photovoltage (> 1.1 V). The increased open-circuit voltage (V_{oc}) is attributed to a reduced non-radiative recombination, as suggested by electroluminescence efficiency and photoluminescence lifetime measurements.

Glass slides with patterned indium tin oxide (ITO) were first coated by vacuum deposition with MoO_3 (5 nm) and a 10 nm thick layer of *N*4,*N*4,*N*4″,*N*4″-tetra([1,1′-biphenyl]-4-yl)-[1,1′:4′,1″-terphenyl]-4,4″-diamine (TaTm), used as the hole transport layer (HTL). $MAPbI_{3-x}Cl_x$ films were prepared in a high vacuum chamber, using three different thermal sources, each equipped with a ceramic crucible and a quartz crystal microbalance sensor, as schematically shown in **Figure 1a**.

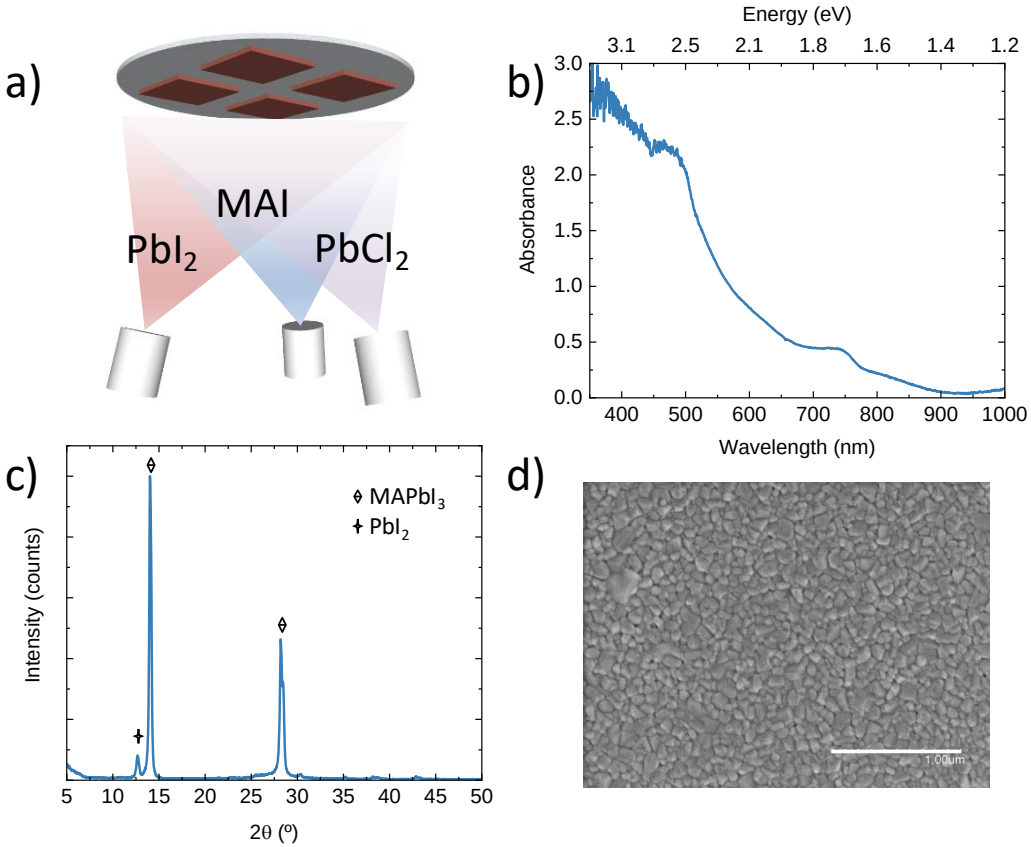

Figure 1. a) Schematics of the three-source vacuum deposition of $MAPbI_{3-x}Cl_x$ thin films. Characterization of perovskite films: b) absorption spectrum, c) XRD pattern and d) SEM image of the sample surface.

Taking into account the reported low solubility of chloride in MAPI,[15] we aimed at the lowest controllable deposition rate for $PbCl_2$ during the process. Hence we fixed the $PbCl_2$ deposition rate at 0.05 Å/s, while PbI_2 was deposited at a rate of 0.6 Å/s. The MAI source was instead maintained at a fixed temperature (85 ºC). After deposition, films were annealed in a nitrogen-filled glove box at 100 ºC for different times. In order to assess whether chloride is retained into the film or is eliminated through the annealing process, we analyzed the sample surface by X-ray photoemission spectroscopy (XPS). As shown in Figure S1 in the Supplementary Information, we did identify chloride on the surface of the samples, in a concentration approximately 10 times lower than iodide ($MAPbI_{3-x}Cl_x$ with $x \approx 0.3$), which correlates with the ratios between the deposition rate of $PbCl_2$ and PbI_2. We have to note, however, that the

Cl2p electrons (with binding energy of 200 eV) have an inelastic mean free path of about 0.8 nm, which translate into a depth of analysis of approximately 2-3 nm.[21] Hence we cannot exclude a different composition within the bulk of the perovskite film. The optical absorption spectrum (Figure 1b) shows the expected profile for MAPI, with an onset at about 780 nm (approximately 1.6 eV). The X-ray diffraction pattern reveals the presence of a small amount of unreacted PbI_2 in the films (12.7º, Figure 1c), as often observed for similar $MAPbI_3$ perovskite materials. However, the diffraction pattern for the tetragonal perovskite structure is clearly visible (main peaks at 14.0°, 28.2°), indicating that indeed highly crystalline $MAPbI_{3-x}Cl_x$ films can be obtained with our technique. The top view scanning electron microscopy (SEM, Figure 1d) shows highly uniform and pin-hole free films, with grain size in the order of hundreds of nanometers. These features are very similar to previously reported vacuum deposited $MAPbI_3$ layers.[22]

The mixed halide films were further tested in a thin film optoelectronic device, by vacuum processing of the electron transport layers (ETLs). They consist of a bilayer of C_{60} fullerene (25 nm) and bathocuproine (BCP, 8 nm), capped with a silver electrode (100 nm).

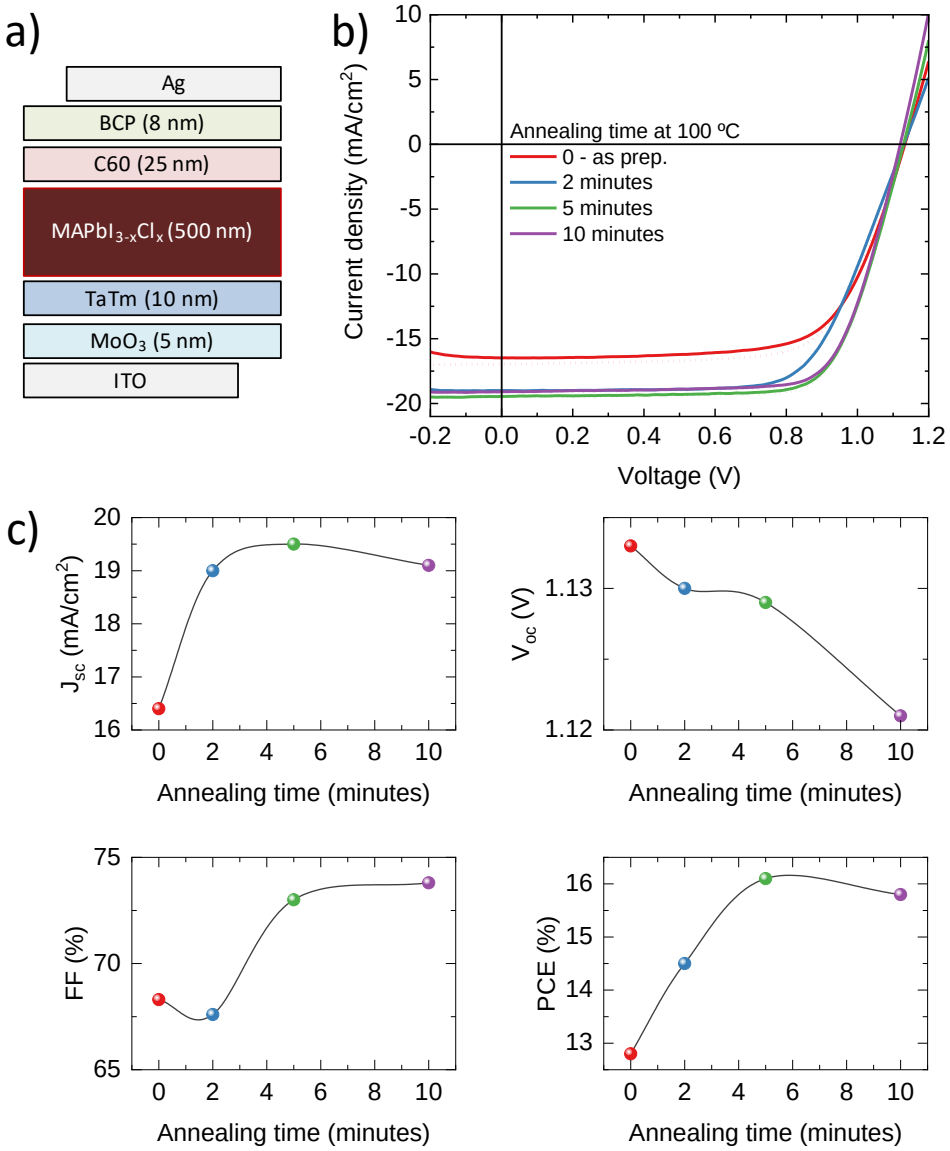

Figure 2. a) Scheme of the vacuum deposited perovskite diode and b) its electrical characterization for different perovskite annealing temperatures; J-V curve under simulated solar illumination are reported in forward (from short to open circuit, solid lines) and in reverse (from open to short circuit, dots) scan. c) Summary of the photovoltaic parameters as a function of the annealing time at 100 ºC.

The perovskite diodes were characterized under AM1.5G simulated illumination. We initially studied the trend of the photovoltaics parameters as a function of the $MAPbI_{3-x}Cl_x$ annealing

time, as shown in **Figure 1**. The current density vs. voltage (J-V) curves (Figure 2a) show good rectification and a marked trend with increasing annealing time. As-prepared samples show unusually low current density (16.4 mA/cm^2), accompanied by a relatively low FF (68%). It is worth to note that the V_{oc} is as high as 1.13 V, about 30 to 50 mV higher compared to state-of-the-art vacuum deposited MAPI solar cells.[22,23] Annealing the perovskite film for 2 minutes, results in an enhancement of the photocurrent (J_{sc} = 19.0 mA/cm^2), with only minor losses in terms of V_{oc} and FF. Longer annealing (5 minutes) substantially recovers the charge collection efficiency (FF = 73%), leading to an overall PCE of 16.1%. Further annealing mainly reduces the photovoltage, which is however still remarkable (1.12 V) for this type of absorber.

The best performing diode was further characterized in forward bias and in an integrating sphere, in order to quantify its electroluminescence efficiency (**Figure 3**). The current density vs. voltage profile (Figure 3a) shows a low current leakage at low bias, with steep injection between 0.6 and 1.1 V, indicating a high diode quality. EL is detected at approximately 1.0 V, rising fast to reach approximately 500 µW/cm^2 at 2.0 V applied bias. This corresponds to an external quantum efficiency (EQE) for EL of 0.3%, which is on a par with the highest performing vacuum deposited MAPI diodes to date.[22]

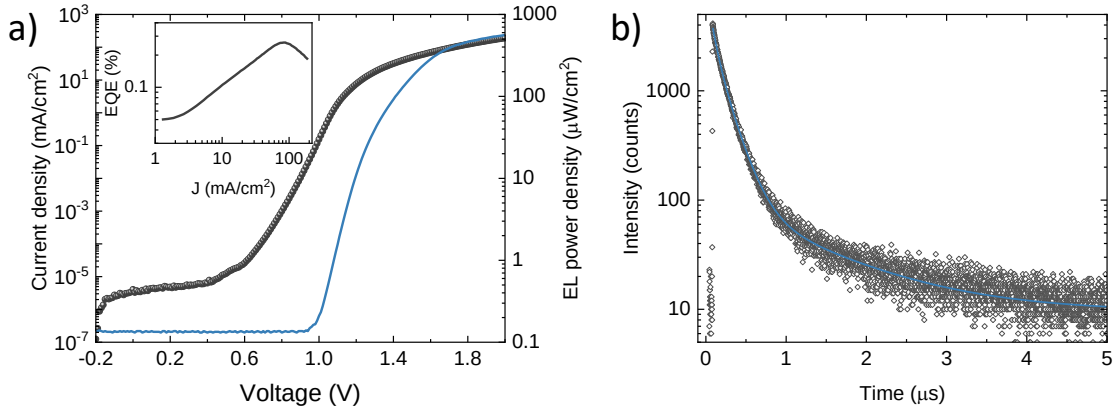

Figure 3. a) Current density (symbols) and electroluminescence power density (line) vs. the applied voltage for a $MAPbI_{3-x}Cl_x$ perovskite diode. Inset shows the EQE for

electroluminescence as a function of the injected current density. b) Photoluminescence lifetime for a $MAPbI_{3-x}Cl_x$ film on glass, upon laser excitation at 375 nm. Raw data are symbols; the line is a fit with a multi-exponential function.

The observation of a high EQE for electroluminescence suggests that the non-radiative recombination pathways are strongly suppressed by incorporation of chloride, in agreement with the literature on similar solution-processed perovskite films.[12] The lower non-radiative recombination might be caused by a reduction in the concentration of trap states, as a result of the incorporation of chloride at grain boundaries.[24] Hence we measured the time-resolved photoluminescence (TRPL) of $MAPbI_{3-x}Cl_x$ films on quartz to investigate the charge recombination dynamics. Figure 3b shows the TRPL trace measured at the maximum of the PL signal upon excitation with a picosecond-fast laser at 375 nm. The measured PL decay kinetics were fitted with a triexponential function of time, obtaining an average PL lifetime of 147 ns (see Supplementary Information for details). The measured lifetime is one order of magnitude longer as compared to previously reported, vacuum deposited, pure MAPI films,[25,26] which are typically characterized by very short PL lifetimes (< 10 ns). Interestingly, the first fast component of the PL decay kinetics has a time constant of 63 ns, similar to previously reported dual-source vacuum deposited $MAPbI_{3-x}Cl_x$ thin films.[27] The fastest decay observed in our materials might be related to different structural/morphological features, and also to the use of UV excitation, which preferentially probes surface recombination. While care should be taken in deducing optoelectronic properties from TRPL, the longer PL lifetime suggests a reduction of the trap density, or the presence of shallower trap states compared to pure MAPI.[28] These observations are consistent with the improvement in device performance, specifically enhanced V_{oc}, using the mixed halide perovskite layers, resulting from a decrease of non-radiative electron-hole recombination channels upon chloride incorporation.

In summary, we showed the formation of the mixed halide $MAPbI_{3-x}Cl_x$ perovskite by means of simultaneous co-evaporation of the three precursors. Films showed good crystallinity and homogeneous morphology, a benchmark of vacuum-deposited perovskite film. We investigated the optoelectronic properties of the material by employing in thin-film diodes. Under illumination, the photovoltage is increased as compared to pure vacuum-processed $MAPbI_3$, reaching 1.13 V and power conversion efficiency exceeding 16%. In forward bias we detected intense electroluminescence with quantum yield of 0.3%, similar to state-of-the-art evaporated perovskite solar cells. These observations, together with the long photoluminescence lifetime, make mixed halide perovskite a good candidate for efficient single junction solar cells and NIR LEDs. Future studies will focus on the optimization of the materials in order to achieve higher power conversion efficiency in both applications.

Experimental Section

Thin film and device preparation: ITO-coated glass substrates were cleaned using soap, water and isopropanol in an ultrasonic bath, followed by UV-ozone treatment. The substrates were transferred into a vacuum chamber integrated into a nitrogen-filled glovebox (H_2O and O_2 < 0.1 ppm) and evacuated to a pressure lower than 10^{-6} mbar. Three quartz crystal microbalance (QCM) sensors were used to monitor the deposition rate of the individual sources. For thickness calibration, we individually sublimed precursors, charge transport materials and their dopants, comparing the thickness inferred from the QCM sensors with that measured using a mechanical profilometer. MoO_3 and TaTm layers were deposited at rates of 0.1 Å/s and 0.4 Å/s, respectively. The evaporation rates of the perovskite precursors were controlled by separate QCM sensors and adjusted to the desired deposition rate, with temperatures ranging from 265-285 ºC for $PbCl_2$ and approximately 290-310 ºC for PbI_2. The crucible containing MAI was kept at a fixed temperature of 85 ºC. After deposition of the perovskite film, C_{60} was evaporated at a rate of 0.4 Å/s with the source temperature at 380 ºC, and subsequently a thin layer (8 nm)

of BCP was sublimed at a rate of 0.3 Å/s with the source temperature of 150 ºC. The devices were finished by deposition of the silver as the top contact (100 nm thick).

Thin-film and device characterization: X-ray diffraction was measured with a Panalytical Empyrean diffractometer equipped with Cu-Kα anode operated at 45 kV and 30 mA and a Pixcel 1D detector in scanning line mode. Single scans were acquired in 2 theta = 10º to 50º range in Bragg-Brentano geometry in air. Anti-scatter slits of 1/16º and step-sizes of 0.025º were used for high-resolution diffractograms. Data analysis was performed with HighScore Plus software. Scanning Electron Microscopy (SEM) images were performed on a Hitachi S-4800 microscope operating at an accelerating voltage of 20 kV over Platinum - metallized samples. Absorption spectra were collected using a fiber-optics based Avantes Avaspec2048 spectrometer. For the solar cell characterization, the J–V characteristics were obtained using a solar simulator by Abet Technologies (model 10500 with an AM1.5G xenon lamp as the light source). Before each measurement, the exact light intensity was determined using a calibrated Si reference diode equipped with an infrared cutoff filter (KG-3, Schott). The J–V curves were recorded between −0.2 V and 1.2 V with 0.01 V steps, integrating the signal for 20 ms after a 10 ms delay. This corresponds to a speed of about 0.3 V s^{-1}. The electroluminescence characterization was carried out using a Keithley Model 2400 source measurement unit and a sensitive Si-photodiode coupled to an integrating sphere. Lifetime measurements (time-correlated single photon counting, TCSPC) were performed using an Edinburgh Instruments FLS1000 Spectrometer. The instrument was equipped with a double emission monochromator, TCSPC electronics, visible PMT detector, and a pulsed diode laser (EPL-375) as the excitation source. TCSPC decays were fitted using the standard Marquardt-Levenberg tail fit algorithm in the Fluoracle software package. A 3-component exponential decay model was used for the fit.

Supporting Information

Supporting Information is available from the Wiley Online Library or from the author.

Acknowledgements

Financial support is acknowledged from the Spanish Ministry of Economy and Competitiveness (MINECO) via the Unidad de Excelencia María de Maeztu MDM-2015-0538, MAT2017-88821-R, PCIN-2015-255, PCIN-2017-014, and the Generalitat Valenciana (Prometeo/2016/135). M.S. thanks the MINECO for his RyC contract. Financial support is acknowledged from the Scientific and Technological Research Council of Turkey (TUBITAK) under the contract number of 315M360.

References

[1] T. M. Brenner, D. A. Egger, L. Kronik, G. Hodes, D. Cahen, *Nat. Rev. Mater.* **2016**, *1*, 15007.

[2] W. Li, Z. Wang, F. Deschler, S. Gao, R. H. Friend, A. K. Cheetham, *Nat. Rev. Mater.* **2017**, *2*, 16099.

[3] J. Huang, Y. Yuan, Y. Shao, Y. Yan, *Nat. Rev. Mater.* **2017**, *2*, 17042.

[4] M. A. Green, E. D. Dunlop, D. H. Levi, J. Hohl-Ebinger, M. Yoshita, A. W. Y. Ho-Baillie, *Prog. Photovoltaics Res. Appl.* **2019**, *27*, 565.

[5] K. Lin, J. Xing, L. N. Quan, F. P. G. de Arquer, X. Gong, J. Lu, L. Xie, W. Zhao, D. Zhang, C. Yan, W. Li, X. Liu, Y. Lu, J. Kirman, E. H. Sargent, Q. Xiong, Z. Wei, *Nature* **2018**, *562*, 245.

[6] W. Xu, Q. Hu, S. Bai, C. Bao, Y. Miao, Z. Yuan, T. Borzda, A. J. Barker, E. Tyukalova, Z. Hu, M. Kawecki, H. Wang, Z. Yan, X. Liu, X. Shi, K. Uvdal, M. Fahlman, W. Zhang, M. Duchamp, J.-M. Liu, A. Petrozza, J. Wang, L.-M. Liu, W. Huang, F. Gao, *Nat. Photonics* **2019**, *13*, 418.

[7] B. Zhao, S. Bai, V. Kim, R. Lamboll, R. Shivanna, F. Auras, J. M. Richter, L. Yang, L. Dai, M. Alsari, X.-J. She, L. Liang, J. Zhang, S. Lilliu, P. Gao, H. J. Snaith, J. Wang,

N. C. Greenham, R. H. Friend, D. Di, *Nat. Photonics* **2018**, *12*, 783.

[8] Z. Li, T. R. Klein, D. H. Kim, M. Yang, J. J. Berry, M. F. A. M. van Hest, K. Zhu, *Nat. Rev. Mater.* **2018**, *3*, 18017.

[9] J. Ávila, C. Momblona, P. P. Boix, M. Sessolo, H. J. Bolink, *Joule* **2017**, *1*, 431.

[10] P. Luo, S. Zhou, W. Xia, J. Cheng, C. Xu, Y. Lu, *Adv. Mater. Interfaces* **2017**, *4*, 1600970.

[11] M. M. Lee, J. Teuscher, T. Miyasaka, T. N. Murakami, H. J. Snaith, *Science (80-.).* **2012**, *338*, 643.

[12] S. D. Stranks, G. E. Eperon, G. Grancini, C. Menelaou, M. J. P. Alcocer, T. Leijtens, L. M. Herz, A. Petrozza, H. J. Snaith, *Science (80-.).* **2013**, *342*, 341.

[13] S. Colella, E. Mosconi, P. Fedeli, A. Listorti, F. Gazza, F. Orlandi, P. Ferro, T. Besagni, A. Rizzo, G. Calestani, G. Gigli, F. De Angelis, R. Mosca, *Chem. Mater.* **2013**, *25*, 4613.

[14] S. Colella, E. Mosconi, G. Pellegrino, A. Alberti, V. L. P. Guerra, S. Masi, A. Listorti, A. Rizzo, G. G. Condorelli, F. De Angelis, G. Gigli, *J. Phys. Chem. Lett.* **2014**, *5*, 3532.

[15] M. Bouchard, J. Hilhorst, S. Pouget, F. Alam, M. Mendez, D. Djurado, D. Aldakov, T. Schülli, P. Reiss, *J. Phys. Chem. C* **2017**, *121*, 7596.

[16] M. Liu, M. B. Johnston, H. J. Snaith, *Nature* **2013**, *501*, 395.

[17] Y. Liu, K. Feng, R.-H. Hsieh, X. Mo, *Mater. Lett.* **2019**, *239*, 163.

[18] J. Jang, G. Choe, S. Yim, *ACS Appl. Mater. Interfaces* **2019**, *11*, acsami.9b05101.

[19] G. Longo, C. Momblona, M.-G. La-Placa, L. Gil-Escrig, M. Sessolo, H. J. Bolink, *ACS Energy Lett.* **2018**, *3*, 214.

[20] L. Gil-Escrig, C. Momblona, M. G. La-Placa, P. P. Boix, M. Sessolo, H. J. Bolink, *Adv. Energy Mater.* **2018**, *8*, 1.

[21] P. J. Cumpson, *J. Electron Spectros. Relat. Phenomena* **1995**, *73*, 25.

[22] C. Momblona, L. Gil-Escrig, E. Bandiello, E. M. Hutter, M. Sessolo, K. Lederer, J. Blochwitz-Nimoth, H. J. Bolink, *Energy Environ. Sci.* **2016**, *9*, 3456.

[23] D. Pérez-del-Rey, L. Gil-Escrig, K. P. S. Zanoni, C. Dreessen, M. Sessolo, P. P. Boix, H. J. Bolink, *Chem. Mater.* **2019**, DOI 10.1021/acs.chemmater.9b01396.

[24] M. Abdi-Jalebi, Z. Andaji-Garmaroudi, S. Cacovich, C. Stavrakas, B. Philippe, J. M. Richter, M. Alsari, E. P. Booker, E. M. Hutter, A. J. Pearson, S. Lilliu, T. J. Savenije, H. Rensmo, G. Divitini, C. Ducati, R. H. Friend, S. D. Stranks, *Nature* **2018**, *555*, 497.

[25] J. B. Patel, R. L. Milot, A. D. Wright, L. M. Herz, M. B. Johnston, *J. Phys. Chem. Lett.* **2016**, *7*, 96.

[26] I. Levine, S. Gupta, A. Bera, D. Ceratti, G. Hodes, D. Cahen, D. Guo, T. J. Savenije, J. Ávila, H. J. Bolink, O. Millo, D. Azulay, I. Balberg, *J. Appl. Phys.* **2018**, *124*, 103103.

[27] C. Wehrenfennig, M. Liu, H. J. Snaith, M. B. Johnston, L. M. Herz, *J. Phys. Chem. Lett.* **2014**, *5*, 1300.

[28] V. S. Chirvony, S. González-Carrero, I. Suárez, R. E. Galian, M. Sessolo, H. J. Bolink, J. P. Martínez-Pastor, J. Pérez-Prieto, *J. Phys. Chem. C* **2017**, *121*, 13381.

The first example of mixed MAPbI3-xClx thin films prepared by three-source vacuum deposition is presented. Increased electroluminescence efficiency and longer photoluminescence lifetimes are observed in the presence of chloride, suggesting a reduction of the non-radiative charge recombination. As a consequence, the photovoltage is increased as compared to vacuum processed chloride-free perovskites, reaching 1.13 V.

Keyword halide perovskites, solar cells, vacuum deposition, mixed halide perovskite

A. Babaei, W. Soltanpoor, M. A. Tesa-Serrate, S. Yerci, M. Sessolo* and H. J. Bolink

Preparation and characterization of mixed halide $MAPbI_{3-x}Cl_x$ perovskite thin films by three-source vacuum deposition.